Nonsteroidal Anti-inflammatory Drug-Activated Gene-1 Expression Inhibits Urethane-Induced Pulmonary Tumorigenesis in Transgenic Mice

Maria Cekanova,[1] Seong-Ho Lee,[1] Robert L. Donnell,[1] Mugdha Sukhthankar,[1] Thomas E. Eling,[2] Susan M. Fischer[3] and Seung Joon Baek[1]

Abstract The expression of nonsteroidal anti-inflammatory drug-activated gene-1 (*NAG-1*) inhibits gastrointestinal tumorigenesis in *NAG-1* transgenic mice (C57/BL6 background). In the present study, we investigated whether the NAG-1 protein would alter urethane-induced pulmonary lesions in *NAG-1* transgenic mice on an FVB background (*NAG-1*$^{Tg+/FVB}$). *NAG-1*$^{Tg+/FVB}$ mice had both decreased number and size of urethane-induced tumors, compared with control littermates (*NAG-1*$^{Tg+/FVB}$ = 16 ± 4 per mouse versus control = 20 ± 7 per mouse, $P < 0.05$). Urethane-induced pulmonary adenomas and adenocarcinomas were observed in control mice; however, only pulmonary adenomas were observed in *NAG-1*$^{Tg+/FVB}$ mice. Urethane-induced tumors from control littermates and *NAG-1*$^{Tg+/FVB}$ mice highly expressed proteins in the arachidonic acid pathway (cyclooxygenases 1/2, prostaglandin E synthase, and prostaglandin E_2 receptor) and highly activated several kinases (phospho-Raf-1 and phosphorylated extracellular signal-regulated kinase 1/2). However, only urethane-induced p38 mitogen-activated protein kinase (MAPK) phosphorylation was decreased in *NAG-1*$^{Tg+/FVB}$ mice. Furthermore, significantly increased apoptosis in tumors of *NAG-1*$^{Tg+/FVB}$ mice compared with control mice was observed as assessed by caspase-3/7 activity. In addition, fewer inflammatory cells were observed in the lung tissue isolated from urethane-treated *NAG-1*$^{Tg+/FVB}$ mice compared with control mice. These results paralleled *in vitro* assays using human A549 pulmonary carcinoma cells. Less phosphorylated p38 MAPK was observed in cells overexpressing NAG-1 compared with control cells. Overall, our study revealed for the first time that the NAG-1 protein inhibits urethane-induced tumor formation, probably mediated by the p38 MAPK pathway, and is a possible new target for lung cancer chemoprevention.

Lung cancer is the leading cause of cancer-related death in men and women in the United States, and pulmonary adenocarcinoma is the most common type of lung cancer, according to the American Cancer Society. Rodents develop chemically induced lung tumors with molecular and histologic features similar to pulmonary adenocarcinoma in humans (1–4). In animal models of lung adenocarcinoma, including rodents, urethane has been used as a carcinogen that specifically induces the development of lung tumors from alveolar type II pneumocytes and Clara cells (2, 4–6).

Nonsteroidal anti-inflammatory drug–activated gene-1 (*NAG-1*) is highly induced by many drugs and chemicals that influence development of tumorigenesis. Also known as a macrophage inhibitory cytokine-1, growth and differentiation factor-15, placental transforming growth factor β, prostate-derived factor, and placental bone morphogenetic protein (7), the NAG-1 protein shows broad activities in various tissues. However, its molecular mechanisms, the receptor, or molecules interacting with NAG-1 are incompletely characterized. As previously published by our group and others, NAG-1 has anti-inflammatory, antiproliferative, and proapoptotic effects in several types of cancer *in vitro* (8–10) and is induced by certain drugs and chemicals. These include nonsteroidal anti-inflammatory drugs (8), chemopreventive dietary compounds (11–14), and peroxisome proliferator activated receptor γ ligands (15–17). Furthermore, NAG-1 is an important downstream target of the tumor suppressor gene *p53* (11), EGR-1 (18), and the PI3K/AKT/GSK-3β pathways (19). Thus, NAG-1 plays a pivotal role in antitumorigenesis induced by chemopreventive compounds.

Authors' Affiliations: [1]Department of Pathobiology, College of Veterinary Medicine, The University of Tennessee, Knoxville, Tennessee; [2]Laboratory of Molecular Carcinogenesis, National Institute of Environmental Health Sciences, NIH, Research Triangle Park, North Carolina; and [3]Department of Carcinogenesis, Science Park-Research Division, The University of Texas M. D. Anderson Cancer Center, Smithville, Texas

Received 1/9/09; revised 3/27/09; accepted 3/31/09; published OnlineFirst 4/28/09.

Grant support: American Cancer Society grant CNE-111611, NIH grant RO1CA108975, The University of Tennessee Center of Excellence in Livestock Diseases and Human Health (S.J. Baek), and National Institute of Environmental Health Sciences/NIH intramural research program (T.E. Eling).

Requests for reprints: Seung Joon Baek, Department of Pathobiology, College of Veterinary Medicine, The University of Tennessee, Knoxville, TN 37996. Phone: 865-974-8216; Fax: 865-974-5616; E-mail: sbaek2@utk.edu.

doi:10.1158/1940-6207.CAPR-09-0057

Transgenic mice (*NAG-1*$^{Tg+/BL6}$) expressing human NAG-1 have been developed by our group (9) and we have found that *NAG-1*$^{Tg+/BL6}$ mice are resistant to chemically and genetically induced intestinal polyp formation. An approximately 50% reduction in polyps was observed after azoxymethane treatment of *NAG-1*$^{Tg+/BL6}$ and 40% inhibition of polyp formation in the intestine by crossing *NAG-1*$^{Tg+/BL6}$ mice with *Apc*$^{Min+}$ mice, compared with control littermates. These results indicate that NAG-1 is a potential tumor suppressor gene in colorectal cancers (9). Because a BL6 background model is not susceptible to chemically induced lung cancer, we have back-crossed *NAG-1*$^{Tg+/BL6}$ mice with the FVB background to generate the NAG-1 transgenic mice with the FVB background (*NAG-1*$^{Tg+/FVB}$) and investigated whether the expression of human NAG-1 would suppress urethane-induced pulmonary adenocarcinoma formation in a mice model. There are a few studies examining a potential role of NAG-1 in lung tumorigenesis (20, 21), based on data showing the down-regulation of NAG-1 expression in lung tumors compared with normal tissue.

In this report, we describe the role of NAG-1 as an antitumorigenic protein in tumors in a urethane-induced mice model. The overexpressed human NAG-1 protein in *NAG-1*$^{Tg+/FVB}$ mice inhibited the formation of lung tumors through down-regulation of the p38 mitogen-activated protein kinase (MAPK) signaling pathway and induced apoptosis through the activation of caspase-3/7. In addition, we have confirmed our findings *in vitro* using human A549 pulmonary carcinoma cells. A decreased phosphorylation of p38 MAPK was observed in cells overexpressing NAG-1 compared with the control cells after various treatments. Data from this study strongly suggest that the NAG-1 protein and its signaling pathway could be potential new targets for prevention and/or treatment of lung cancer.

Materials and Methods

Reagents, antibodies, and cells

Urethane was purchased from Sigma-Aldrich; cigarette smoke condensate was obtained from Murty Pharmaceuticals, Inc.; epidermal growth factor (EGF) and insulin-like growth factor-1 (IGF-I) were purchased from BD Biosciences; and prostaglandin E_2 (PGE_2) was purchased from Cayman Chemical Co. NAG-1 antibody was previously described (8). Microsomal PGE_2 synthase antibody was purchased from Oxford Biomedical Research, and lysozyme antibody was purchased from Dako North America, Inc. Antibodies for cyclooxygenase (COX)-2, cyclin D1, p27, p53, and actin were purchased from Santa Cruz Biotechnology. COX-1 and EP_2 antibodies were obtained from Cayman Chemical Co. Phospho-Raf-1 (Ser^{259}), phospho-p38 MAPK (Thr^{180}/Tyr^{182}), p21, and cleaved caspase-3 (Asp^{175}) antibodies were purchased from Cell Signaling Technology. Human A549 lung carcinoma cell line was obtained from American Type Culture Collection. The cells were maintained in Ham's F12K medium supplemented with 10% fetal bovine serum and antibiotics (100 IU penicillin and 100 μg/mL streptomycin) and grown in an atmosphere of 5% CO_2 at 37°C.

Animals and experimental design

All animal research procedures were approved by the University of Tennessee Institutional Animal Care and Use Committee and were in accordance with NIH guidelines. NAG-1 transgenic mice were originally developed on a C57BL/6 genetic background (9). *NAG-1*$^{Tg+/BL6}$ mice were backcrossed to FVB strain mice for eight generations. Mice were maintained at 22 ± 2°C on a 12 h light/dark cycle with free access to standard rodent chow and tap water. Eleven-week-old control littermates (*NAG-1*$^{Tg-/FVB}$, $n = 11$) and NAG-1 transgenic mice (*NAG-1*$^{Tg+/FVB}$, $n = 10$) received i.p. injections of urethane (1 mg of urethane dissolved in 0.9% NaCl/g body weight) or 0.9% NaCl alone once per week for 6 wk (Fig. 1A). At age 30 wk, mice were sacrificed and lung tissues were collected and kept in RNa later solution for protein and RNA analysis and in 10% neutral-buffered formalin for paraffin embedding.

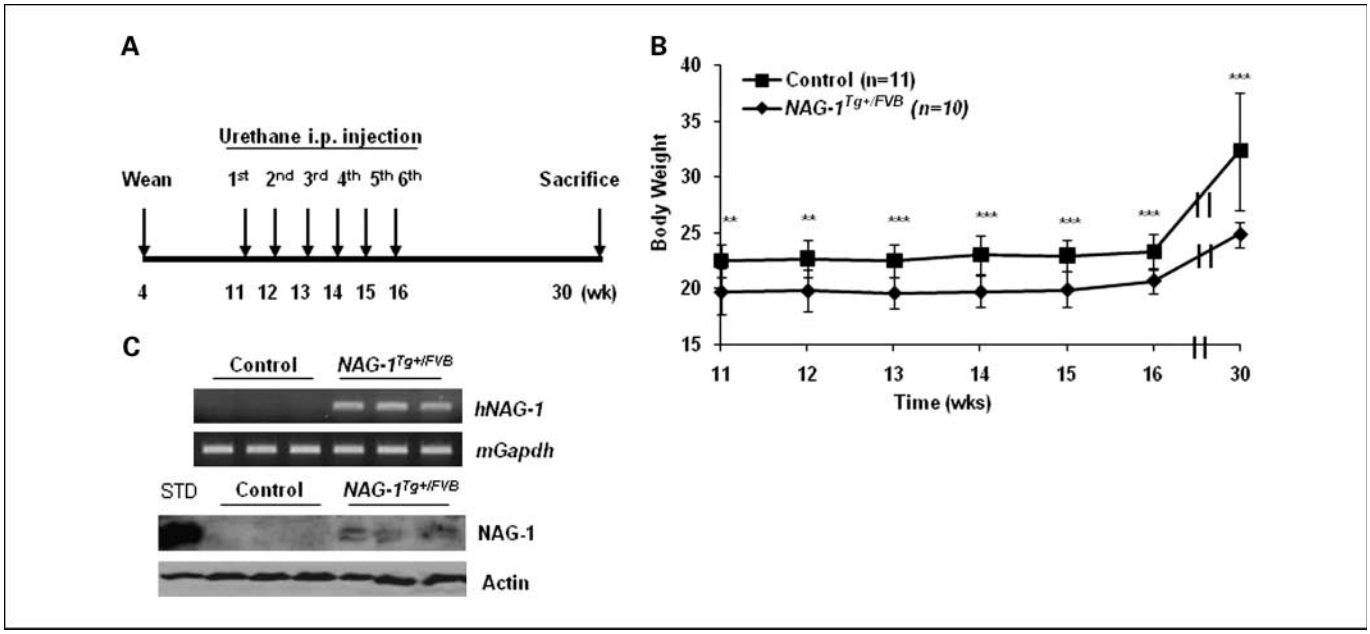

Fig. 1. Characterization of *NAG-1*$^{Tg+/FVB}$ mice. *A*, schematic diagram of the experimental design. *B*, body weight for control and *NAG-1*$^{Tg+/FVB}$ mice (**, $P < 0.01$; ***, $P < 0.001$). *C*, human NAG-1 expression in lung tissue of *NAG-1*$^{Tg+/FVB}$ mice was confirmed by reverse transcription-PCR and Western blotting. Human HCT-116 colorectal cancer cell lysate was used as the standard (*STD*) for human NAG-1 expression.

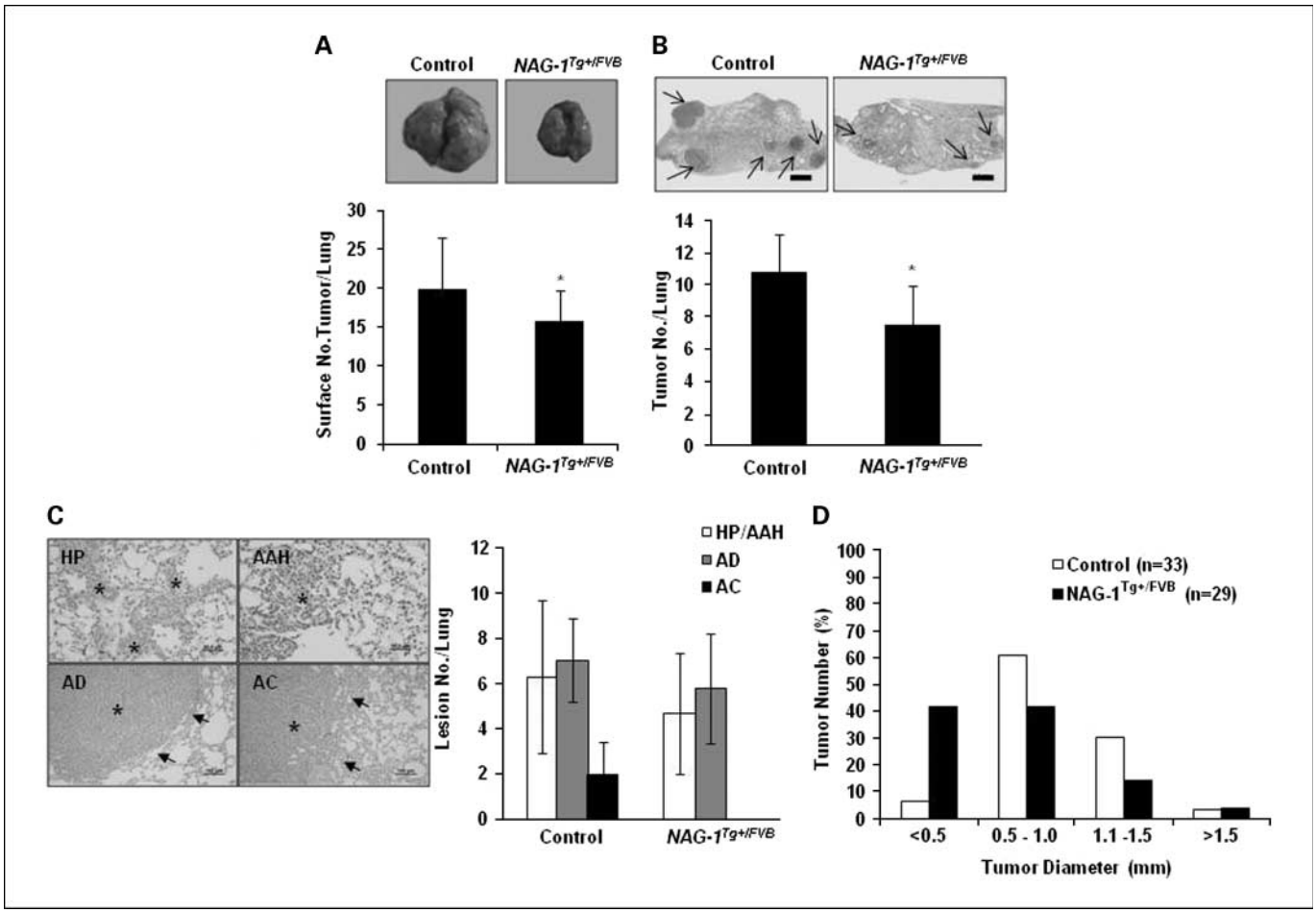

Fig. 2. Suppression of urethane-induced pulmonary neoplasia in *NAG-1*$^{Tg+/FVB}$ mice. *A,* top, images of dissected lungs from control (*left*) and *NAG-1*$^{Tg+/FVB}$ (*right*) mice. The bottom graph shows that *NAG-1*$^{Tg+/FVB}$ mice had a significantly lower gross incidence of urethane-induced pulmonary neoplasia compared with control littermates. Columns, mean of surface tumors from each treatment group; bars, SD. The Student's *t* test was used to analyze the data (*, $P < 0.05$). *B,* top, a representative lung section stained by H&E with pulmonary tumors from control (*left*) and *NAG-1*$^{Tg+/FVB}$ (*right*) mice. Magnification, 20×; scale bar, 1.0 mm. Columns, mean tumor numbers per lung; bars, SD. The Student's *t* test was used to analyze the data (*, $P < 0.05$). *C,* representative images of foci of hyperplasia (*HP, asterisk, top left*), atypical adenomatous hyperplasia (*AAH, asterisk, top right*), multiple adenomas (*AD, asterisk, bottom left*) characterized as well differentiated and compressing the surrounding tissues (*arrows in AD*), and adenocarcinomas (*AC, asterisk, bottom right*) with localized fingering invasion into surrounding parenchyma or airways (*arrows in AC*). Magnification, 400× and 200×; scale bars, 50 and 100 μm, respectively. Graph at right shows evaluation of each type of lesion per lung section of each treatment group. Columns, mean; bars, SD. The Student's *t* test was used to analyze the data. *D,* the distribution of tumor numbers as percentage of total numbers of control ($n = 33$) and $n = 29$ of *NAG-1*$^{Tg+/FVB}$ mice as related to size (diameter, mm). The tumor diameters were divided into four groups according to size (<0.5, 0.5-1.0, 1.1-1.5, and >1.5 mm).

Lung tumor enumeration

Surface (gross) lung lesions were counted by three blinded readers after removing the lung from sacrificed mice. The microscopic evaluation of lung lesions was done using H&E-stained lung tissue slides.

Histology and immunohistochemistry

Lung tissues were formalin fixed, embedded in paraffin, and sectioned at 5 μm. Immunohistochemical staining was done as described previously (3). The images were captured by an Olympus DP70 camera (Olympus Optical Col) attached to an Olympus microscope. For scoring of lysozyme staining in inflammatory cells (22), slides were reviewed by three blinded readers. For each lung specimen ($n = 3$ per treatment group), six normal cross-sectional lung areas, four edge areas of neoplasia, and one central area of neoplasia were evaluated and scored for intensity (1 = weak, 2 = moderate, 3 = intense staining). Scores for number and intensity of staining of inflammatory cells were then multiplied and normalized to the control group.

Measuring the diameter of neoplasia in lungs

To measure the diameter of neoplasia, photographic images (magnification 2×) of the lung lobes were taken. The diameters of the neoplasia were measured by the Olympus software package. For each treatment group, ~30 neoplastic foci were measured and divided into four groups according to size. For evaluation of percentage of cross-sectional area occupied by neoplasia, H&E lung images of each mouse were taken at a magnification of 2× and measured using Scion Image software to compare the area of normal and neoplastic pulmonary tissue. Measured areas of all neoplasia from the same lung were combined, divided by the area of the whole lung, and multiplied by 100 to get a result as a percentage. The results were presented as a mean ± SD for each treatment group, and statistical analyses were done.

Reverse transcription-PCR

Total RNA was isolated from mice lung tissue using an RNeasy mini kit (Qiagen), and then cDNA was synthesized from 1 μg of total RNA using an iScript cDNA Synthesis kit (Bio-Rad) according to the

manufacturer's protocols as described previously (23). The primer sequences used in our study were *h-NAG-1* (F: 5′-CGGAACGAGGGCAACCTGCACAGCC-3′, R: 5′-TATGCAGTGGCAGTCTTTG-3′) and *m-Gapdh* (F: 5′-CAGGAGCGAGACCCCACTAACAT-3′, R: 5′-GTCAGATCCACGACGGACACATT-3′).

Western blot

Lung tissues were homogenized and then sonicated in ice-cold radioimmunoprecipitation assay buffer (1× PBS, 1% NP40, 0.5% sodium deoxycholate, 0.1% SDS) supplemented with protease and phosphatase inhibitors (1 μg/mL aprotinin, 1 μg/mL leupeptin, 1 mmol/L phenylmethylsulfonyl fluoride, 1 mmol/L Na_3VO_4, and 25 mmol/L NaF). Proteins from A549 cells were used for immunoblotting as described previously (24).

Caspase-3/7 activity

The Caspase-Glo 3/7 Assay kit was used to measure apoptosis in mouse lung tissue following the manufacturer's protocol. Briefly, the tissue lysates were prepared using radioimmunoprecipitation assay buffer, and a total of 30 μg of proteins were added into 96-well tissue culture plates with white walls and a clear bottom, and an equal amount of luminescence substrate for caspase-3/7 was added to each sample. After 1-h incubation in the dark at room temperature, the luminescence was measured in a plate-reading luminometer (FLx800) as directed by the manufacturer (BioTek Instruments).

Terminal deoxyribonucleotide transferase–mediated nick-end labeling assay

TACS2 TdT-DAB In Situ Apoptosis detection kit was purchased from Trevigen and used to detect apoptotic cells. Briefly, the lung sections were deparaffinized, rehydrated, and washed in 1× PBS. Samples were incubated in cytonin solution for 30 min at room temperature, washed in 1× PBS, immersed in quenching solution for 5 min, and then washed in 1× PBS. After washing, the slides were immersed in 1× terminal deoxyribonucleotide transferase labeling solution for 5 min followed by incubation in labeling reaction mix for 1 h. Then, the samples were washed with stop buffer and incubated with streptomycin-horseradish peroxidase solution, and the bound conjugate was visualized by 3,3′-diaminobenzidine staining. The samples were counterstained by methyl green staining. As a positive control, we used a lung tissue pretreated with TACS-Nuclease to generate DNA breaks in cells. The results were analyzed under a microscope.

Transient transfection

All transfection experiments were done using Lipofectamine 2000 reagent (Invitrogen Corporation) according to the manufacturer's instructions, as described previously (8) After transfection and serum starvation, the cells were treated with the indicated compounds for 0.5 and 2 h.

Statistical analysis

We used the Student's *t* test and ANOVA test to analyze the data. Results were considered statistically significant at $^{*}P < 0.05$, $^{**}P < 0.01$, and $^{***}P < 0.001$.

Results

Characterization of *NAG-1*$^{Tg+/FVB}$ mice

To explore the role of NAG-1 in lung tumorigenesis, *NAG-1*$^{Tg+/BL6}$ mice were bred with wild FVB strain mice to generate *NAG-1*$^{Tg+/FVB}$ mice, which are a more susceptible model for lung carcinogenesis (22). To evaluate the effects of NAG-1 on lung tumorigenesis, urethane was used to induce pulmonary adenomas and adenocarcinomas in mice (6). Eleven-week-old *NAG-1*$^{Tg+/FVB}$ ($n = 10$) and control littermate mice ($n = 11$) received i.p. injections of urethane or 0.9% NaCl alone once per week for 6 wk. Fourteen weeks after the last urethane treatment, mice were sacrificed and lung tissues were examined and collected for further analysis (Fig. 1A).

NAG-1$^{Tg+/BL6}$ have been reported viable and fertile with no distinguishable behavioral, clinical, or histopathologic phenotype except that the mice had reduced body weight compared with the control littermates (9). A similar decrease in body weight was observed in the *NAG-1*$^{Tg+/FVB}$ compared with control mice (Fig. 1B; *NAG-1*$^{Tg+/FVB}$ = 24.8 ± 1.1 g per mouse versus control = 32.3 ± 5.2 g per mouse at 30 wk, $P < 0.001$). However, the weight of dissected lungs from *NAG-1*$^{Tg+/FVB}$ mice was not significantly reduced compared with lungs from control mice (*NAG-1*$^{Tg+/FVB}$ = 0.219 ± 0.03 g per mouse versus control = 0.245 ± 0.01 g per mouse, $P = 0.14$).

NAG-1 expression in lungs of *NAG-1*$^{Tg+/FVB}$ mice was confirmed by reverse transcription-PCR and Western blotting analysis (Fig. 1C). RNA transcripts of the human *NAG-1* gene were amplified from lung samples of *NAG-1*$^{Tg+/FVB}$ mice, whereas no amplified products were detectable in control mice (Fig. 1C, *top*). Cell lysates from urethane-treated lung tissue were subjected to Western blotting analysis, and the NAG-1 protein was detected only in tissues obtained from the *NAG-1*$^{Tg+/FVB}$ mice (Fig. 1C, *bottom*). NAG-1 expression in *NAG-1*$^{Tg+/FVB}$ mice was also seen in other tissues, including skin, colon, brain, and kidney (data not shown).

NAG-1$^{Tg+/FVB}$ mice had reduced urethane-induced lung lesions

To characterize the urethane-induced lesions, lungs were dissected from mice and evaluated by gross examination and light microscopy. There was a 100% incidence of lung lesions in both the control and *NAG-1*$^{Tg+/FVB}$ mice treated with urethane; however, no lung lesions were observed in saline-treated groups (data not shown). To determine whether NAG-1 expression alters urethane-induced lung tumorigenesis, surface lung tumors were counted (Fig. 2A). The *NAG-1*$^{Tg+/FVB}$ mice had a modest but significantly lower number of urethane-induced pulmonary tumors, compared with the control littermates (*NAG-1*$^{Tg+/FVB}$ = 16 ± 4 per mouse versus control = 20 ± 7 per mouse, $P < 0.05$). The light microscopic examination of multiple lung sections H&E stained with roughly equivalent cross-sectional areas revealed the location of most neoplasia at the periphery of the lungs (Fig. 2B). Lungs from urethane-treated control mice had significantly more lesions compared with urethane-treated *NAG-1*$^{Tg+/FVB}$ mice (*NAG-1*$^{Tg+/FVB}$ = 7.4 ± 2.4 per lung versus control = 10.7 ± 3.8 per lung, $P < 0.05$). No significant pulmonary pathology was observed in the lungs from the saline-treated control mice (data not shown). In the lung sections from the urethane-treated control ($n = 11$) and *NAG-1*$^{Tg+/FVB}$ mice ($n = 9$), foci of hyperplasia (Fig. 2C), atypical adenomatous hyperplasia (Fig. 2C), and multiple pulmonary epithelial neoplasia were present. The majority of the neoplastic foci were considered adenomas (Fig. 2C), characterized by being well-differentiated, compressing the surrounding tissues (Fig. 2C), with no to minimal mitotic activities, and solid to mixed (solid and papillary) architectural pattern. Approximately 20% of the neoplasias in the urethane-induced control mice were considered adenocarcinomas (Fig. 2C) with localized fingering invasion into surrounding parenchyma or airways, and with an average mitotic index of 3.2 mitotic figures per 40× objective

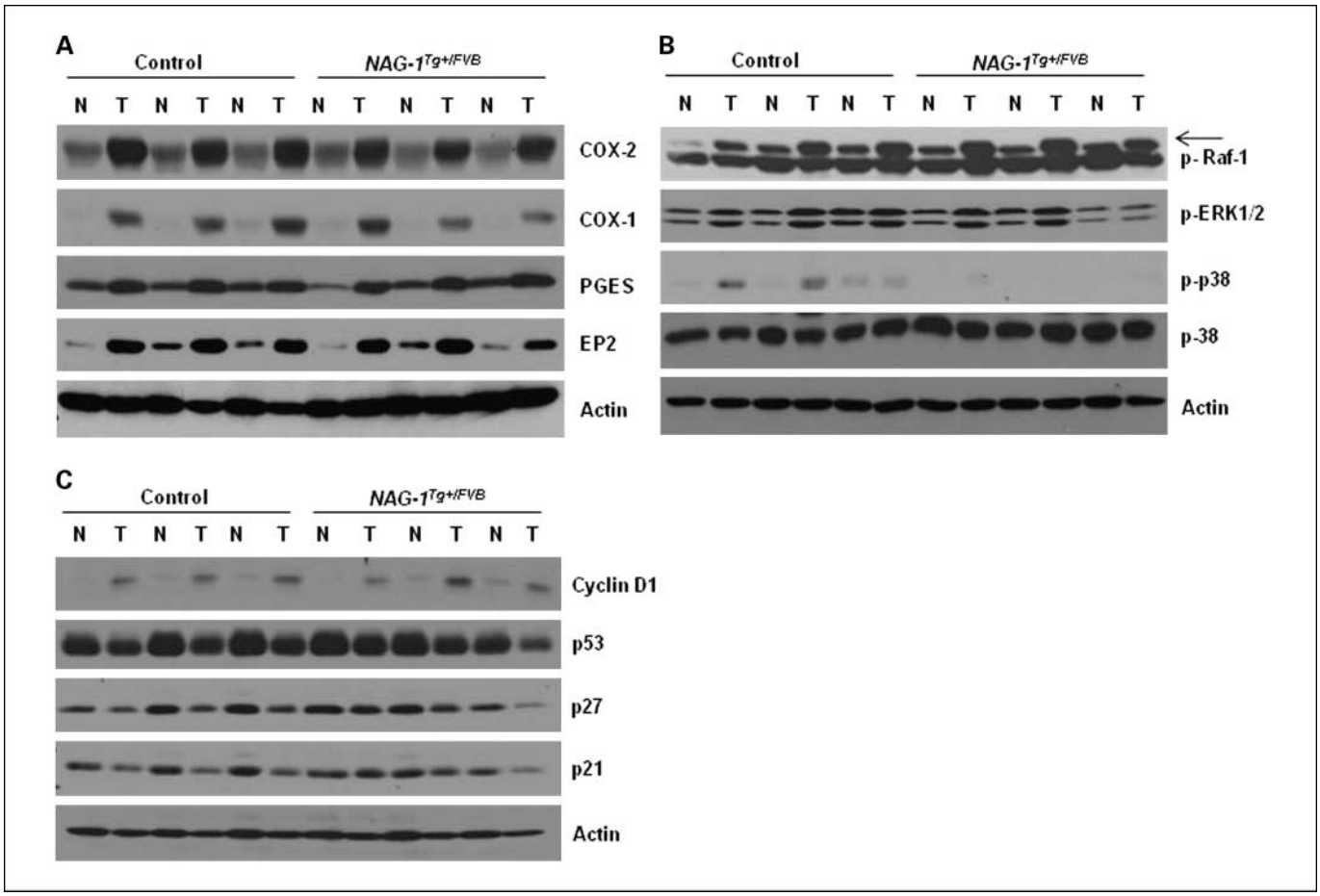

Fig. 3. p38 MAPK signaling pathway is affected by NAG-1 in urethane-treated lung tissue. *A*, lung tumors (*T*) and adjacent normal tissues (*N*) were isolated from three representative control and *NAG-1*$^{Tg+/FVB}$ mice and were subjected to Western blotting analysis using the antibodies for COX-1, COX-2, PGE_2 synthase (PGES), and EP2 expression. *B*, expression of phospho-Raf-1, phosphorylated extracellular signal-regulated kinase 1/2 (p-ERK1/2), and phospho-p38 MAPK in lung tissues. Actin and total p38 MAPK antibodies were used as loading controls. *C*, the effect of NAG-1 expression on the cell cycle proteins and tumor suppressor protein p53.

field; however, no metastasis was observed. Interestingly, no adenocarcinomas were identified in lung sections from the urethane-treated *NAG-1*$^{Tg+/FVB}$ mice (n = 10). The results are based on analysis of the sections from lung lobes of each mouse; thus, obtained data are from only a limited area of the lung. Approximately the same areas were analyzed from the each treatment group. The diameters of tumors from the *NAG-1*$^{Tg+/FVB}$ mice (n = 29) were compared with the diameters of neoplasia from the control littermates (n = 33). Most of the tumors of the control mice were >0.5 mm in size, whereas 58% of *NAG-1*$^{Tg+/FVB}$ mice had lung tumors with diameters more than 0.5 mm in size (Fig. 2D). In general, the tumors in the *NAG-1*$^{Tg+/FVB}$ mice were smaller than the tumors in the control mice. Overall, *NAG-1*$^{Tg+/FVB}$ mice had reduced tumor amount and size, with no adenocarcinomas compared with control littermates, indicating the possible role of NAG-1 in inhibition of lung tumor progression.

Phospho-38 MAPK is affected by NAG-1 in urethane-induced lung tumorigenesis

To further characterize the effects of the NAG-1 protein on lung tumorigenesis and to identify possible mechanisms involved in pulmonary tumor growth and progression, we examined protein expression in lung tissue from urethane-treated *NAG-1*$^{Tg+/FVB}$ and control mice. Proteins of the arachidonic acid pathway play important roles in lung tumorigenesis (25) and several proteins involved in this pathway were examined. The expression of COX-2, COX-1, and PGE_2 synthase was up-regulated in lung tumor tissues from both treated control and *NAG-1*$^{Tg+/FVB}$ mice (Fig. 3A). The expression of EP2 and EP4, two members of the prostaglandin E receptor family, were also examined; however, we were not able to detect EP4 receptor expression in mice lung tissue (data not shown). In contrast, the EP2 receptor was highly expressed in lung tumor tissues from both *NAG-1*$^{Tg+/FVB}$ and control mice. The expression of several other signaling proteins involved in lung tumorigenesis was examined. The active Raf-1 and extracellular signal-regulated kinase 1/2 play an important role in lung tumorigenesis (24, 26, 27), and an increased activation of Raf-1 and extracellular signal-regulated kinase 1/2 was observed in tumor tissue from both *NAG-1*$^{Tg+/FVB}$ and control mice (Fig. 3B). We also examined cell cycle–related proteins, including cyclin D1, p53, p27, and p21. However, as shown in Fig. 3C, the expression of these proteins was not affected by NAG-1 overexpression.

Urethane-induced phosphorylation of p38 MAPK at Thr^{180}/Tyr^{182} was increased in tumor tissue compared with normal

tissue from control mice. In contrast, the phosphorylation of p38 MAPK was significantly lower in tumor and normal tissue isolated from *NAG-1*$^{Tg+/FVB}$ mice, suggesting that the expression of NAG-1 inhibits phosphorylation of p38 MAPK (Fig. 3B). There were no significant differences in *NAG-1*$^{Tg+/FVB}$ and control mice in the expression of either phospho-AKT or phosphorylated stress-activated protein kinase/c-Jun-NH_2-kinase (data not shown). Our data suggest that NAG-1 expression may cause alteration of p38 MAPK in urethane-induced lung tumorigenesis.

Immunohistochemical analysis was also done to confirm and localize protein expression in the pulmonary tissues. Using an antibody specific for the phosphorylated form of p38 MAPK at Thr^{180}/Tyr^{182}, there was a substantial decrease in staining intensity for the active p38 MAPK in nuclei and cytoplasm in the lung tumors of *NAG-1*$^{Tg+/FVB}$ mice (data not shown).

NAG-1 protein activates apoptosis in urethane-induced pulmonary adenomas

It has been reported that NAG-1 induces caspase activity (28). To evaluate the possible involvement of NAG-1 in regulating lung tumorigenesis through apoptosis, caspase-3/7 activities in normal and tumor tissues of the lungs were measured. The caspase-3/7 activities in lung tumors were highly significantly increased in *NAG-1*$^{Tg+/FVB}$ mice, compared with control mice and with the normal lung of *NAG-1*$^{Tg+/FVB}$ mice (Fig. 4A). There was no significant difference in caspase-3/7 activities between the normal lungs from control and *NAG-1*$^{Tg+/FVB}$ mice.

To further show that the NAG-1 protein modulates apoptotic pathways in lung tumorigenesis, the lung tissues were treated with an antibody specifically recognizing only the cleaved form of caspase-3. Immunohistochemical staining was positive for active caspase-3, localized to the cytoplasm in the tumors of *NAG-1*$^{Tg+/FVB}$ mice, but not in the tumors of control mice (data not shown). The appearance of apoptosis was confirmed by terminal deoxyribonucleotide transferase–mediated nick-end labeling (TUNEL) assay as shown in Fig. 4B.

NAG-1 protein inhibits urethane-induced inflammation

In addition to the role of NAG-1 in antitumorigenesis, it has been shown that NAG-1 affects anti-inflammatory activity by reducing tumor necrosis factor-α secretion in macrophages (29). Urethane- or cigarette smoke–induced lung tumor formation may be potentiated by inflammation (22, 30). To check the role of NAG-1 in inflammation, we performed immunohistochemical staining of lysozyme to detect the presence of inflammatory cells in lung tissue. Lysozyme is an enzyme highly expressed in cytoplasmic granules of the granulocytic series of inflammatory cells, such as macrophages and polymorphonuclear neutrophils (Fig. 5A). As shown in Fig. 5B, *NAG-1*$^{Tg+/FVB}$ mice had a significant 50% reduced number of lysozyme-positive cells in the lung over control mice ($P < 0.05$). Thus, this suggests that NAG-1 suppresses urethane-induced inflammation in lung tissue.

Inhibition of p38 MAPK phosphorylation in human A549 lung carcinoma cells by NAG-1 overexpression

To verify the role of the NAG-1 protein in inhibition of lung tumors in *NAG-1*$^{Tg+/FVB}$ mice through the p38 MAPK, human

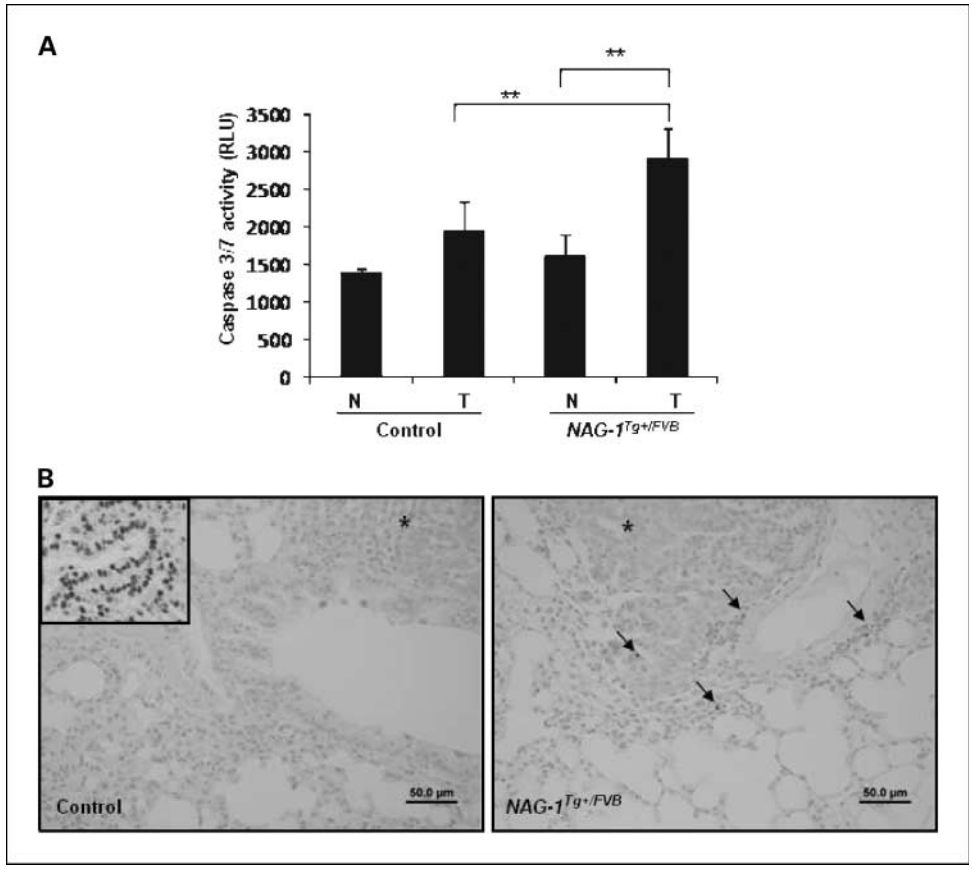

Fig. 4. The NAG-1 protein activates apoptosis in urethane-induced pulmonary tumors. *A,* normal and tumor tissue from control and *NAG-1*$^{Tg+/FVB}$ mice were subjected to caspase-3/7 activity assay. RLU, relative luciferase units. Columns, mean from three different mice; bars, SD; **, $P < 0.01$. *B,* TUNEL assay of control (*left*) and *NAG-1*$^{Tg+/FVB}$ (*right*) mice. Inset, positive control. Asterisks, pulmonary adenomas; arrows, positively brown stained cells. Magnification, 400×; scale bar, 50 μm.

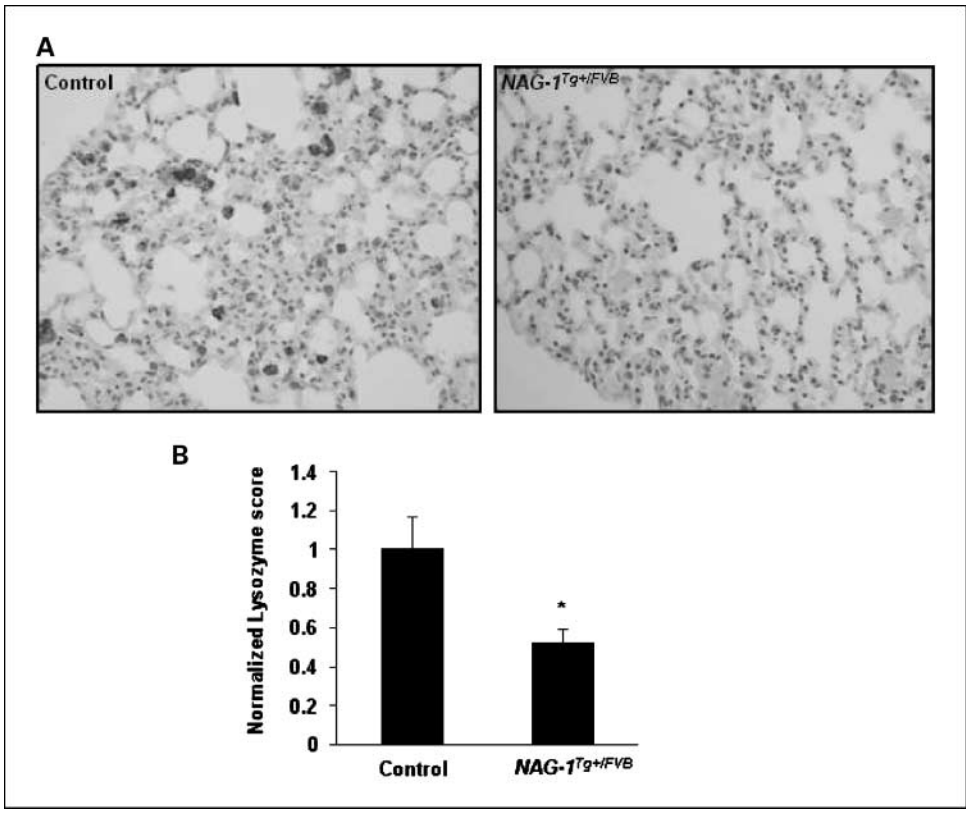

Fig. 5. NAG-1 inhibits urethane-induced inflammation. *A*, immunohistochemical analysis of lysozyme marker in lung tissues from control and *NAG-1*$^{Tg+/FVB}$ mice. Hematoxylin was used as counterstain. Magnification, 400×. *B*, the graph represents the semiquantization of scored intensity. Statistical analyses were done using the Student's *t* test; *, $P < 0.05$.

A549 lung carcinoma cells were transiently transfected with a plasmid construct containing the human *NAG-1* gene. After transfection, A549 cells were treated with 12-*O*-tetradecanoylphorbol-13-acetate (20 nmol/L), cigarette smoke condensate (40 μg/mL), EGF (100 nmol/L), IGF-I (100 nmol/L), and PGE_2 (50 nmol/L) for 0.5 and 2 h. As shown in Fig. 6A, treatment with cigarette smoke condensate had the ability to induce phosphorylation of p38 MAPK at 2 h and its expression was diminished in the presence of the NAG-1 protein. Similar results were observed when A549 cells were treated with both growth factors EGF and IGF-I, as well with inflammatory cytokine PGE_2 (Fig. 6B and C). Interestingly, the NAG-1 protein had no effect on the phosphorylation of p38 MAPK after treatment with 12-*O*-tetradecanoylphorbol-13-acetate (Fig. 6A). In addition, the NAG-1 protein had no effect on the phosphorylation of p42/p44 MAPK after activation by all tested agents in transiently transfected A549 cells (data not shown).

Discussion

NAG-1 has antiproliferative and proapoptotic effects in several types of cancer *in vitro* and is highly induced by many chemopreventive compounds (7). NAG-1 is highly expressed in normal tissue of the small intestine and it is significantly reduced in human colorectal carcinomas and neoplastic intestinal polyps of *Apc*$^{Min+}$ mice (31). In the human lung, NAG-1 was reported to be highly expressed in normal tracheobronchial epithelium, but absent in several tumor tissues from adenoma, small cell, large cell, and squamous cell carcinomas (20). Those findings are in agreement with observations in this study, in which the expression of the human NAG-1 protein plays an important role in lung tumorigenesis.

NAG-1 transgenic mice on a C57BL/6J background were generated using the Cre/LoxP system (9). *NAG-1*$^{Tg+/BL6}$ mice were viable and fertile with no apparent phenotype other than a reduction in body weight compared with nontransgenic littermate controls. In this study, we generated *NAG-1*$^{Tg+/FVB}$ mice because the FVB strain is a more susceptible model for urethane-induced lung tumorigenesis. With more than eight generations of backcross with wild-type mice with FVB background, we found that body weight was still less in *NAG-1*$^{Tg+/FVB}$ mice compared with the control mice (Fig. 1B), indicating that NAG-1–induced body weight reduction is seen not only in C57BL/6J mice but also in other strains of mice.

It has been known that urethane-induced lung tumors in rodents provide an excellent model to determine the efficacy of tumor suppressor genes as a preventative method, as well to evaluate mechanisms responsible for antitumorigenesis. This experimental system can be vigorously examined throughout lung carcinogenesis, from the appearance of early preneoplastic proliferative lesions and small adenomas to malignancy. Urethane-induced pulmonary adenomas predominantly occur in the periphery of the lung (2, 4, 6). Primary mouse lung tumors share morphologic, histologic, and molecular characteristics with human lung tumors. Our data suggest that *NAG-1*$^{Tg+/FVB}$ mice had a significantly lower incidence of urethane-induced pulmonary lesions compared with the control littermates, with the localization of most neoplasia at the periphery of the lungs. Histology of the lung sections from urethane-treated control and *NAG-1*$^{Tg+/FVB}$ mice revealed the formation of hyperplasia and pulmonary epithelial neoplasia (Fig. 2C). Nearly all neoplasia were considered adenomas, but only in the control mice, urethane also induced

adenocarcinomas with typical invasion into surrounding tissue. However, no adenocarcinomas were observed in the lung tissue sections from *NAG-1*$^{Tg+/FVB}$ mice. Based on these data, NAG-1 may play a role in inhibition of malignancy in lung tumorigenesis. Similarly, another study suggests that NAG-1 expression induces the differentiation of normal tracheobronchial epithelium (20), although the defined biological role of the NAG-1 protein in the epithelium is not yet fully understood.

Chronic inflammation is linked to carcinogenesis in several organ systems, including the colon and lung, and inflammatory cells increase expression of factors that may support the growth, angiogenesis, and metastasis of cancer cells. The p38 MAPK activation is well associated with extracellular matrix remodeling, inflammation, and contractile dysfunction of the heart (32). However, the role of p38 MAPK in tumorigenesis depends on cell type and stimuli (33). In contrast to a number of publications discussing the role of the p38 MAPK pathway as antitumorigenic, many publications have provided evidence for its role in the progression of tumorigenesis via increasing production of proinflammatory cytokines. For example, recently published results by Stathopoulos et al. (22) showed that urethane-induced lung tumor formation is initiated by inflammation through the activation of nuclear factor-κB. Another study shows that mice, after exposure to cigarette smoke, show increased lung inflammatory cell influx, activation of nuclear factor-κB and p38 MAPK, and increased levels of matrix metalloproteinase-9 and proinflammatory cytokines, such as tumor necrosis factor-α and interleukin-6 (30). Because NAG-1 appears to have anti-inflammatory activity by reducing tumor necrosis factor-α secretion in macrophages (29) and p38 MAPK was inactivated in the *NAG-1*$^{Tg+/FVB}$ mice after urethane exposure, our data indicated that p38 MAPK could be a novel downstream target of the NAG-1 signaling pathway, resulting in the reduction of inflammatory cells (Fig. 5) and potentially leading to inhibition of the lung tumorigenesis. The importance of NAG-1 in lung tumorigenesis was confirmed by *in vitro* experiments. Our data revealed that cigarette smoke condensate–, IGF-I–, EGF-, or PGE_2-induced phosphorylation of p38 MAPK was down-regulated in the presence of overexpressed NAG-1 in human A549 lung carcinoma cells (Fig. 6A-C).

Western blot for NAG-1 in A549 cells (Fig. 6) and in mice lung tissue (Fig. 1C) revealed two bands that migrate as a doublet (35 kDa) on SDS-PAGE gels. This phenomenon was observed in other cell lines, such as human LNCaP prostate carcinoma cells (34). We speculated that the *NAG-1* gene has

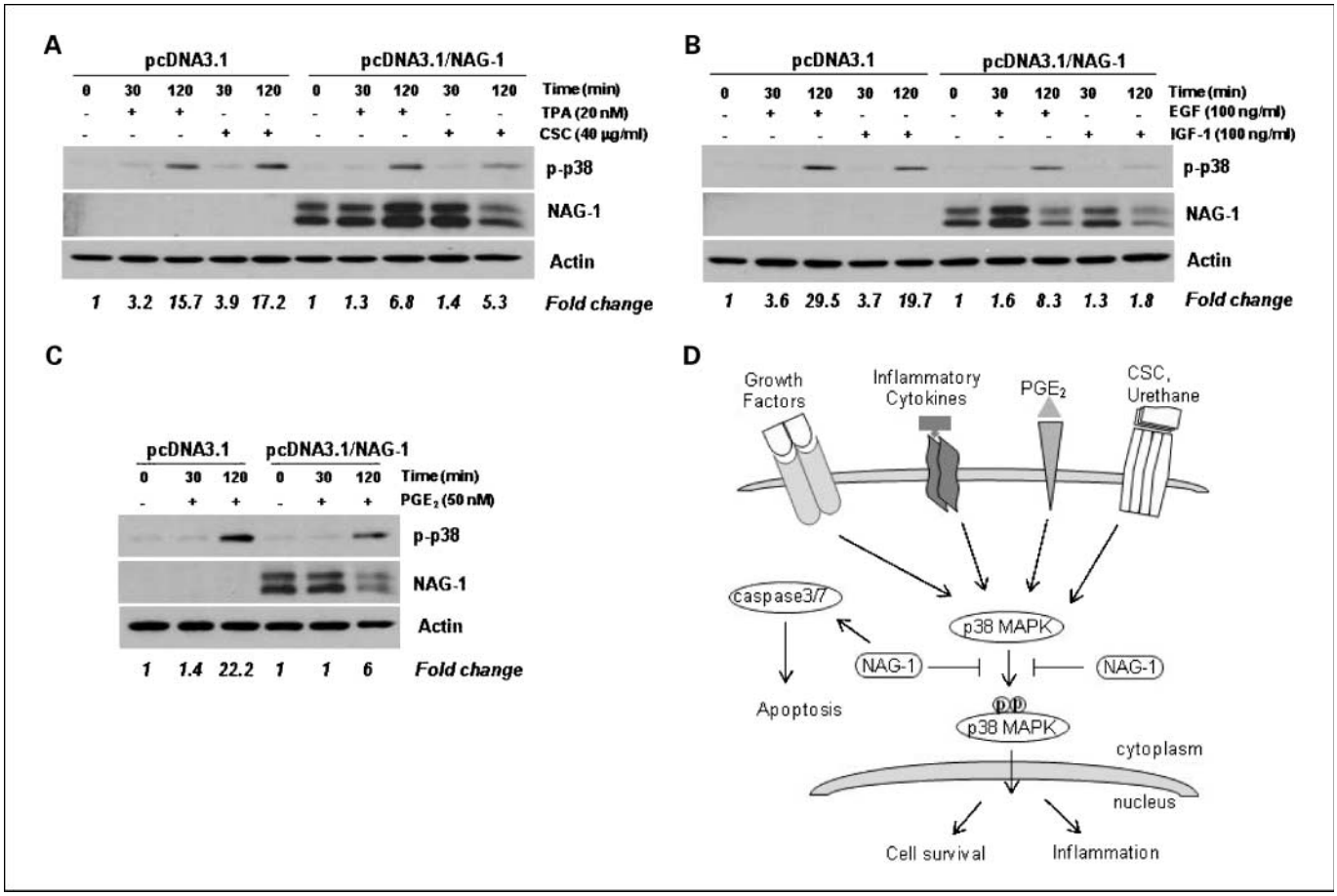

Fig. 6. NAG-1 inhibits phosphorylation of p38 MAPK in A549 cells. A549 cells were grown and transiently transfected with empty or pcDNA3.1/NAG-1 expression vector. After transfection, A549 cells were treated with 20 nmol/L 12-*O*-tetradecanoylphorbol-13-acetate (*TPA*) and 40 μg/mL cigarette smoke condensate (*CSC*; *A*), 100 ng/mL EGF and 100 ng/mL IGF-I (*B*), or 50 nmol/L PGE_2 (*C*) for 30 and 120 min. The phosphorylation of p38 MAPK, NAG-1, and actin expression was evaluated by Western blotting analysis. The numbers below represent densitometry analysis of phospho-p38 normalized to actin, and then compared with the controls (0 min set as 1.0 in each transfection). *D,* schematic diagram of the role of NAG-1 in lung tumorigenesis.

two translational initiation codons, which produce two different peptides with 13-amino-acid differences. Given that both bands are induced by several anticancer compounds including vitamin D (35), and Western blot with NAG-1 peptide showed disappearance of both bands, we strongly believe that these are from different usage of the translation initiation start site. However, the biological function of the short form is still unknown and needs to be addressed in future studies.

Prevention by eliminating tumor promoters, early diagnosis, and new target treatment are keys to reduce the numbers of deaths caused by lung cancer. In the present study, we propose antitumorigenic activities of NAG-1 in lung cancer. Overexpressed human NAG-1 reduced tumor number and size and protected the progression of urethane-induced pulmonary neoplasia in mouse models. The newly identified NAG-1 downstream molecular target was p38 MAPK. NAG-1 had proapoptotic activity by increasing caspase-3/7 activities. To our knowledge, we have shown for the first time that NAG-1 has anti-inflammatory activity in lungs through the inhibition of inflammatory cells. Our *in vivo* data were also confirmed by *in vitro* data using human A549 lung carcinoma cells overexpressing human NAG-1. We conclude that NAG-1 plays a role as a tumor suppressor gene in lung tumorigenesis, and the elucidation of NAG-1 downstream signaling can help us to better understand the regulation of lung cancer prevention (Fig. 6D).

Disclosure of Potential Conflicts of Interest

No potential conflicts of interest were disclosed.

Acknowledgments

We thank Misty R. Bailey (University of Tennessee) for her critical reading of the manuscript, Dr. Michael F. McEntee for valuable suggestions, and Dr. Heon-Suk Lee and Xiuoon Li for their technical assistance.

References

1. Stearman RS, Dwyer-Nield L, Zerbe L, et al. Analysis of orthologous gene expression between human pulmonary adenocarcinoma and a carcinogen-induced murine model. Am J Pathol 2005;167:1763–75.
2. Nikitin AY, Alcaraz A, Anver MR, et al. Classification of proliferative pulmonary lesions of the mouse: recommendations of the mouse models of human cancers consortium. Cancer Res 2004;64:2307–16.
3. Schuller HM, Cekanova M. NNK-induced hamster lung adenocarcinomas over-express β2-adrenergic and EGFR signaling pathways. Lung Cancer 2005;49:35–45.
4. Bauer AK, Dwyer-Nield LD, Malkinson AM. High cyclooxygenase 1 (COX-1) and cyclooxygenase 2 (COX-2) contents in mouse lung tumors. Carcinogenesis 2000;21:543–50.
5. Mason RJ, Kalina M, Nielsen LD, Malkinson AM, Shannon JM. Surfactant protein C expression in urethane-induced murine pulmonary tumors. Am J Pathol 2000;156:175–82.
6. Meyer AM, Dwyer-Nield LD, Hurteau GJ, et al. Decreased lung tumorigenesis in mice genetically deficient in cytosolic phospholipase A2. Carcinogenesis 2004;25:1517–24.
7. Baek SJ, Eling TE. Changes in gene expression contribute to cancer prevention by COX inhibitors. Prog Lipid Res 2006;45:1–16.
8. Baek SJ, Kim KS, Nixon JB, Wilson LC, Eling TE. Cyclooxygenase inhibitors regulate the expression of a TGF-β superfamily member that has proapoptotic and antitumorigenic activities. Mol Pharmacol 2001;59:901–8.
9. Baek SJ, Okazaki R, Lee SH, et al. Nonsteroidal anti-inflammatory drug-activated gene-1 overexpression in transgenic mice suppresses intestinal neoplasia. Gastroenterology 2006;131:1553–60.
10. Li PX, Wong J, Ayed A, et al. Placental transforming growth factor-β is a downstream mediator of the growth arrest and apoptotic response of tumor cells to DNA damage and p53 overexpression. J Biol Chem 2000;275:20127–35.
11. Baek SJ, Wilson LC, Eling TE. Resveratrol enhances the expression of non-steroidal anti-inflammatory drug-activated gene (NAG-1) by increasing the expression of p53. Carcinogenesis 2002;23:425–34.
12. Lee SH, Kim JS, Yamaguchi K, Eling TE, Baek SJ. Indole-3-carbinol and 3,3′-diindolylmethane induce expression of NAG-1 in a p53-independent manner. Biochem Biophys Res Commun 2005;328:63–9.
13. Baek SJ, Kim JS, Jackson FR, Eling TE, McEntee MF, Lee SH. Epicatechin gallate-induced expression of NAG-1 is associated with growth inhibition and apoptosis in colon cancer cells. Carcinogenesis 2004;25:2425–32.
14. Lee SH, Cekanova M, Baek SJ. Multiple mechanisms are involved in 6-gingerol-induced cell growth arrest and apoptosis in human colorectal cancer cells. Mol Carcinog 2008;47:197–208.
15. Yamaguchi K, Lee SH, Eling TE, Baek SJ. A novel peroxisome proliferator-activated receptor γ ligand, MCC-555, induces apoptosis via posttranscriptional regulation of NAG-1 in colorectal cancer cells. Mol Cancer Ther 2006;5:1352–61.
16. Baek SJ, Kim JS, Nixon JB, DiAugustine RP, Eling TE. Expression of NAG-1, a transforming growth factor-β superfamily member, by troglitazone requires the early growth response gene EGR-1. J Biol Chem 2004;279:6883–92.
17. Baek SJ, Wilson LC, Hsi LC, Eling TE. Troglitazone, a peroxisome proliferator-activated receptor γ (PPAR γ) ligand, selectively induces the early growth response-1 gene independently of PPAR γ. A novel mechanism for its anti-tumorigenic activity. J Biol Chem 2003;278:5845–53.
18. Baek SJ, Kim JS, Moore SM, Lee SH, Martinez J, Eling TE. Cyclooxygenase inhibitors induce the expression of the tumor suppressor gene EGR-1, which results in the up-regulation of NAG-1, an antitumorigenic protein. Mol Pharmacol 2005;67:356–64.
19. Yamaguchi K, Lee SH, Eling TE, Baek SJ. Identification of nonsteroidal anti-inflammatory drug-activated gene (NAG-1) as a novel downstream target of phosphatidylinositol 3-kinase/AKT/GSK-3β pathway. J Biol Chem 2004;279:49617–23.
20. Newman D, Sakaue M, Koo JS, et al. Differential regulation of nonsteroidal anti-inflammatory drug-activated gene in normal human tracheobronchial epithelial and lung carcinoma cells by retinoids. Mol Pharmacol 2003;63:557–64.
21. Chen YL, Lin PC, Chen SP, et al. Activation of NAG-1 via ERK1/2 mitogen-activated protein kinase revealed a isochaihulactone-triggered apoptotic pathway in human lung cancer A549 cells. J Pharmacol Exp Ther 2007;323:746–56.
22. Stathopoulos GT, Sherrill TP, Cheng DS, et al. Epithelial NF-κB activation promotes urethane-induced lung carcinogenesis. Proc Natl Acad Sci U S A 2007;104:18514–9.
23. Cekanova M, Yuan JS, Li X, Kim K, Baek SJ. Gene alterations by peroxisome proliferator-activated receptor γ agonists in human colorectal cancer cells. Int J Oncol 2008;32:809–19.
24. Cekanova M, Majidy M, Masi T, Al-Wadei HA, Schuller HM. Overexpressed Raf-1 and phosphorylated cyclic adenosine 3′-5′-monophosphatate response element-binding protein are early markers for lung adenocarcinoma. Cancer 2007;109:1164–73.
25. Brown JR, DuBois RN. Cyclooxygenase as a target in lung cancer. Clin Cancer Res 2004;10:4266–9s.
26. Majidi M, Al-Wadei HA, Takahashi T, Schuller HM. Nongenomic β estrogen receptors enhance β1 adrenergic signaling induced by the nicotine-derived carcinogen 4-(methylnitrosamino)-1-(3-pyridyl)-1-butanone in human small airway epithelial cells. Cancer Res 2007;67:6863–71.
27. Patek CE, Arends MJ, Wallace WA, et al. Mutationally activated K-ras 4A and 4B both mediate lung carcinogenesis. Exp Cell Res 2008;314:1105–14.
28. Jang TJ, Kim NI, Lee CH. Proapoptotic activity of NAG-1 is cell type specific and not related to COX-2 expression. Apoptosis 2006;11:1131–8.
29. Bootcov MR, Bauskin AR, Valenzuela SM, et al. MIC-1, a novel macrophage inhibitory cytokine, is a divergent member of the TGF-β superfamily. Proc Natl Acad Sci U S A 1997;94:11514–9.
30. Yao H, Edirisinghe I, Rajendrasozhan S, et al. Cigarette smoke-mediated inflammatory and oxidative responses are strain dependent in mice. Am J Physiol Lung Cell Mol Physiol 2008;294:L1174–86.
31. Kim KS, Baek SJ, Flake GP, Loftin CD, Calvo BF, Eling TE. Expression and regulation of nonsteroidal anti-inflammatory drug-activated gene (NAG-1) in human and mouse tissue. Gastroenterology 2002;122:1388–98.
32. Li M, Georgakopoulos D, Lu G, et al. p38 MAP kinase mediates inflammatory cytokine induction in cardiomyocytes and extracellular matrix remodeling in heart. Circulation 2005;111:2494–502.
33. Nebreda AR, Porras A. p38 MAP kinases: beyond the stress response. Trends Biochem Sci 2000;25:257–60.
34. Shim M, Eling TE. Protein kinase C-dependent regulation of NAG-1/placental bone morphogenic protein/MIC-1 expression in LNCaP prostate carcinoma cells. J Biol Chem 2005;280:18636–42.
35. Lambert JR, Kelly JA, Shim M, et al. Prostate derived factor in human prostate cancer cells: gene induction by vitamin D via a p53-dependent mechanism and inhibition of prostate cancer cell growth. J Cell Physiol 2006;208:566–74.